

- Litt, M. H. *J. Polym. Sci., Polym. Chem. Ed.* **1988**, *26*, 3043.
 (o) Schulz, R. C.; Schwarzenbach, E. *Makromol. Chem. Macromol. Symp.* **1988**, *13/14*, 495. (p) Cheradame, H.; Tadjang, A. U.; Gandini, A. *Makromol. Chem., Rapid Commun.* **1988**, *9*, 255.
 (2) Kobayashi, S.; Igarashi, T.; Moriuchi, Y.; Saegusa, T. *Macromolecules* **1986**, *19*, 535.
 (3) Kobayashi, S.; Iijima, S.; Igarashi, T.; Saegusa, T. *Macromolecules* **1987**, *20*, 1729.
 (4) Tomalia, D. A.; Huffines, J. D. U. S. A. Patent 4261925, 1981; *Chem. Abstr.* **1981**, *95*, 535.
 (5) Kobayashi, S.; Shoda, S.; Masuda, E.; Shimano, Y. *Macromolecules* **1989**, *22*, 2878.
 (6) Deslongchamp, P.; Dube, S.; Lebreux, C.; Patterson, D. R.; Taillefer, R. *Can. J. Chem.* **1975**, *53*.
 (7) Kobayashi, S.; Morikawa, K.; Shimizu, N.; Saegusa, T. *Polym. Bull.* **1984**, *11*, 253.
 (8) Witte, H.; Seeliger, W. *Liebigs Ann. Chem.* **1974**, 966.
 (9) Saegusa, T.; Ikeda, H.; Fujii, H. *Polym. J.* **1973**, *4*, 87.
 (10) Meyers, A. I.; Temple, D. L.; Nolen, R. L.; Mihelich, E. D. *J. Org. Chem.* **1974**, *39*, 2778.

Cationic Copolymerizations of Cyclooxaalkanes

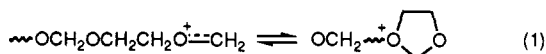
Young-Gu Cheun, C. Peter Lillya, Paul M. Lahti, and James C. W. Chien*

Department of Polymer Science and Engineering and Department of Chemistry,
 University of Massachusetts, Amherst, Massachusetts 01003. Received July 11, 1988;
 Revised Manuscript Received May 22, 1989

ABSTRACT: Cationic copolymerizations of 2-butyl-1,3-dioxepane (= 2-Bu-DOP) with 1,3-dioxolane (= DOL) and with tetrahydrofuran (= THF) have been carried out. The copolymers have T_g 's in accordance with the Fox relationship. The reactivity ratios have been obtained by using Fineman-Ross analysis. The rate constants for 2-Bu-DOP (= a) and DOL (= b) copolymerization at -10°C are $k_{a,a} = 7.1 \times 10^{-4}$, $k_{b,a} = 6.5 \times 10^{-4}$, $k_{a,b} = 3.3 \times 10^{-4}$, and $k_{b,b} = 5.4 \times 10^{-4}$ in units of $(\text{M s})^{-1}$; the corresponding rate constant values at 0°C for the copolymerization of THF (= b) are 3.0×10^{-3} , 8.2×10^{-5} , 9×10^{-4} , and 7.4×10^{-4} $(\text{M s})^{-1}$. The mechanisms of the copolymerizations are discussed.

Introduction

In the polymerization of oxygen heterocyclic compounds, the oxonium structure for the propagating species is widely accepted, i.e. in the case of tetrahydrofuran (= THF).¹ For 1,3-dioxalkanes, the acetal bond is highly reactive and is easily opened in the presence of acid catalysts.² The ΔG_p of cyclic acetal polymerization has small negative or even positive value due to relatively low negative ΔH_p ; consequently the monomer and polymer are in reversible equilibrium.³ Thermodynamic parameters for polymerizations of DOL^{3,4} (= 1,3-dioxolane), 4-Me-DOL,⁵ DOP^{3,4} (= 1,3-dioxepane), 4-Me-DOP,^{6,7} 2-Me-DOP,^{6,7} TOC^{4b,8,9} (= 1,3,6-trioxocane), and 2-Bu-TOC have been reported. Because of the stabilizing effect of the α -oxygen atom, alkoxy carbenium, C^+ , ions are in equilibrium with the cyclic oxonium ion, O^+ . This is illustrated for DOL



Either ionic species can participate in propagation.

Penczek et al.¹ have argued that in the case of DOL the O^+ ion is the dominant propagating species. The fact that 2- and 4-Me-DOL's¹⁰ form only oligomers seem to be consistent with a steric effect in the O^+ mechanism. However, recent observations that 2-alkyl derivatives of DOP⁷ and TOC⁹ polymerize at the same or faster rates than the unsubstituted monomers suggest the intermediacy of alkoxy carbenium ions in propagation. The central objective of this work is to investigate the copolymerizations of THF and DOL, which are both thought to polymerize via the cyclic oxonium ion, with 2-Bu-

DOP, which may involve an alkoxy carbenium ion as a propagating species.

Experimental Section

Materials. 2-Bu-DOP was prepared by the reaction of 1,4-butanediol and valeraldehyde¹¹ in the presence of a Dowex 50-X8-100 ion-exchange resin as previously described.⁷ THF, DOL, triethylamine, methylene chloride, and 1,2-dichloroethane from Aldrich were purified by usual procedures. Boron trifluoride etherate was distilled immediately before use.

Copolymerizations. Copolymerization was carried out in a Schlenk tube equipped with a magnetic stir bar and fitted with a rubber septum. Tubes were flame-dried under vacuum and filled with purified nitrogen. A mixture of monomers dissolved in either methylene chloride or 1,2-dichloroethane was introduced by syringe and equilibrated at the thermostated reaction temperature followed by injection of the catalyst solution. The conversion versus polymerization time was followed by quenching aliquot with a precisely weighed excess amount of triethylamine. A known amount of tetralin was added as the GC standard, and the sample was diluted with solvent. The concentration of unreacted monomer in the mixture was analyzed with GC. The monomer concentrations were calculated from calibration curves previously determined for known mixtures of 2-Bu-DOP/DOL and of 2-Bu-DOP/THF. The copolymers were precipitated by addition of triethylamine, washed with aqueous methanol, and evacuated at 100°C to yield the copolymers.

Methods. An Hewlett-Packard 5790A chromatograph was used for GC using an OV-101 silicone packed column. A Varian Associates XL-200 instrument was used for ^1H NMR. A Perkin-Elmer DSC-II system was used to determine T_g at a $20^\circ\text{C}/\text{min}$ heating rate.

Results

Time Conversion of Polymerizations. The homopolymerization time conversion curves at -10°C are shown

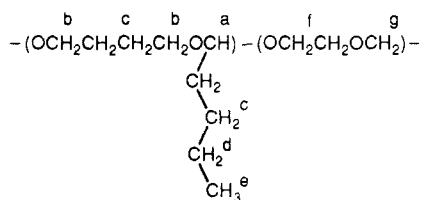
in parts A and B of Figure 1 for 2-Bu-DOP and DOL, respectively. 2-Bu-DOP polymerizes slightly faster than DOL, reaching equilibrium in ca. 30 h as compared to 45 h for the latter. Comparison of the homopolymerizations of 2-Bu-DOP and THF in Figure 2 showed the former to be about 37-fold faster than the latter at 0 °C. At this temperature the equilibrium was reached in ca. 10 h for 2-Bu-DOP polymerization. There was no induction period in any of these homopolymerizations nor in the copolymerizations (vide infra). This is in contrast to the long induction periods reported for the polymerizations of DOL^{4b} and DOP¹² initiated with $\text{Et}_3\text{O}^+\text{BF}_4^-$. THF polymerized to only 8% conversion and its $[M]_{e,T}$ is 4.67 M. Subscripts T, P, and L are used to denote THF, 2-Bu-DOP, and DOL, respectively. The results of copolymerizations of 2-Bu-DOP with DOL and THF are given in Figures 3 and 4, respectively. The rate of conversion of 2-Bu-DOP and of DOL in the copolymerizations is slower than in homopolymerizations. However, the opposite is true in the case of THF monomer, which was consumed much faster in copolymerizations with 2-Bu-DOP than in its homopolymerization. The rate constant of propagation (k_p) was obtained from the slope of plot for

$$\ln \left(\frac{M_0 - M_e}{M_t - M_e} \right) = k_p [c] t \quad (2)$$

where $[M]_0$, $[M]_t$, and $[M]_e$ are the monomer concentrations at times zero and t and at equilibrium, respectively, and $[c]$ is the catalyst concentration. Figure 5 illustrates this kinetic analysis for the homopolymerizations of 2-Bu-DOP and of DOL at -10 °C. The values of $[M]_e$ and k_p are summarized in Table I.

Copolymer Structures. Copolymerizations were conducted to low conversions for a range of feed ratios. The conditions employed for 2-Bu-DOP/DOL copolymerizations at -10 °C are given in Table II.

Figure 6 is a typical ¹H NMR spectrum for a 2-Bu-DOP/DOL copolymer containing 25 mol % of DOL. It has six resonance signals centered at 0.87, 1.29, 1.60, 3.39, 3.56, and 4.42 ppm from TMS, the assignments for which are



From the intensities of the peaks at 0.87, 3.39, 3.56, and 4.42 ppm, the composition of the copolymers were obtained and given in column 6 of Table II.

Several DSC curves for 2-Bu-DOP/DOL copolymers are shown in Figure 7. The T_g values thus obtained are plotted against copolymer composition in Figure 8.

2-Bu-DOP/THF copolymerizations over a wide range of comonomer feed ratios were performed. The copolymerization conditions at -10 and 0 °C are given in Tables III and IV, respectively.

¹H NMR is used to determine the 2-Bu-DOP and THF contents in the copolymers. Figure 9 is a typical spectrum for a polymer containing about 20% THF. The spectra are characterized by six resonance signals centered at 0.85, 1.26, 1.60, 3.37, 3.53, and 4.41 ppm from

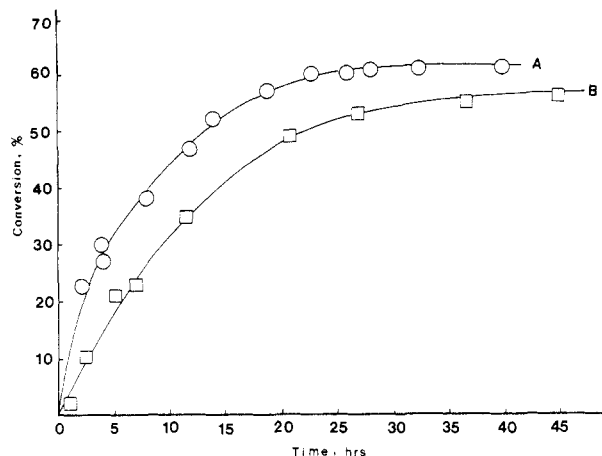


Figure 1. Homopolymerization time conversion curves at -10 °C using methylene chloride as the solvent and $\text{BF}_3 \cdot \text{Et}_2\text{O}$ (31 mM) as the initiator: (A) 2-Bu-DOP, initial concentration = 4.8 M; (B) DOL, initial concentration = 4.9 M.

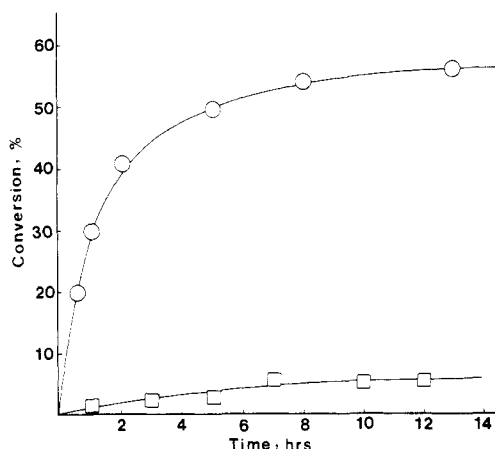
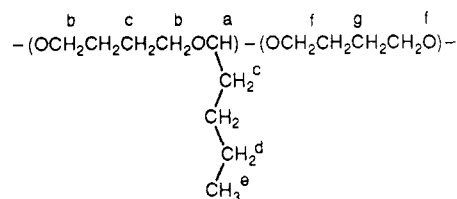


Figure 2. Homopolymerization time conversion curves at 0 °C using methylene chloride as the solvent and $\text{BF}_3 \cdot \text{Et}_2\text{O}$ (31 mM) as the initiator: (O) 2-Bu-DOP, initial concentration = 4.8 M; (□) THF, initial concentration = 5.1 M.

TMS, which are assigned as follows:



The compositions of the copolymers are obtained from the intensities of the resonance peaks at 1.60, 3.37, 3.52, and 4.41 ppm and given in column 6 of Tables III and IV.

The T_g of 2-Bu-DOP/THF copolymers were determined by DSC; the results of several samples are shown in Figure 10. Figure 11 is a plot of T_g versus copolymer composition.

Discussion of Results

The copolymers of 2-Bu-DOP and THF have T_g values that are related to the $T_{g,P}$ and $T_{g,T}$ of the homopolymers according to the Fox equation¹²

$$\frac{1}{T_g} = \frac{W_P}{T_{g,P}} + \frac{W_T}{T_{g,T}} \quad (3)$$

where W_P and W_T are the weight fraction of 2-Bu-DOP

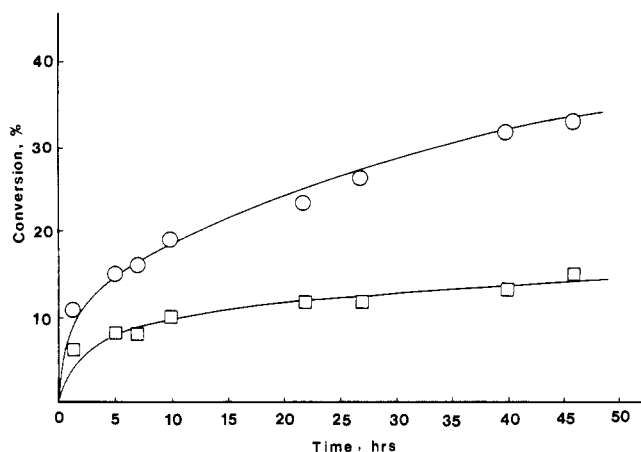


Figure 3. Time conversion curves for 2-Bu-DOP/DOL copolymerizations at -10°C using methylene chloride as the solvent and $\text{BF}_3\cdot\text{Et}_2\text{O}$ (10.9 mM) as the initiator: (O) 2-Bu-DOP conversion, initial concentration = 4.96 M; (\square) DOL conversion, initial concentration = 5.13 M.

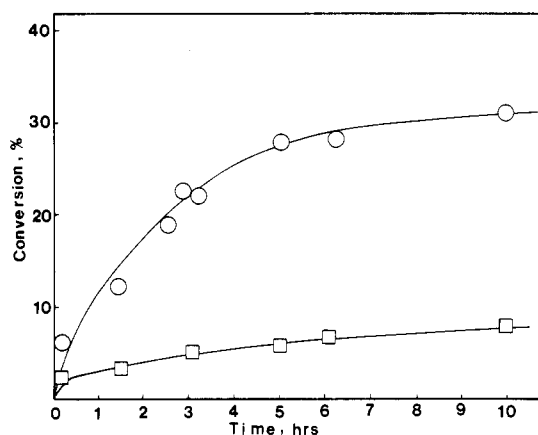


Figure 4. Time conversion curves for 2-Bu-DOP/THF copolymerization at 0°C using methylene chloride as the solvent and $\text{BF}_3\cdot\text{Et}_2\text{O}$ (10.9 mM) as the initiator: (O) 2-Bu-DOP conversion, initial concentration = 5.0 M; (\square) THF conversion, initial concentration = 4.94 M.

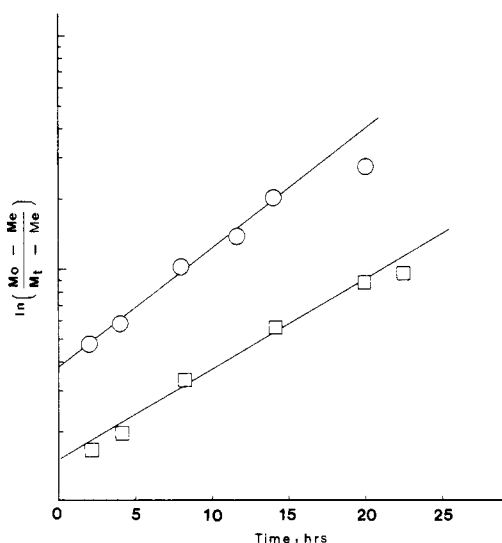


Figure 5. Kinetic analysis of the data in Figure 1: (O) 2-Bu-DOP; (\square) DOL.

and THF, respectively. Table V compares the calculated (eq 3) and observed T_g values. The solid curve in Figure 10 is the curve for the Fox equation which fits

Table I
Homopolymerization Results^a

monomer	temp, $^{\circ}\text{C}$	$[\text{M}]_0$, M	k_p , $(\text{M s})^{-1}$
2-Bu-DOP	-10	1.87	7.1×10^{-4}
DOL	-10	1.55	6.5×10^{-4}
2-Bu-DOP	0	2.1	3.0×10^{-3}
THF	0	4.67	8.2×10^{-5}

^a Conditions: catalyst, $\text{BF}_3\cdot\text{O}(\text{C}_2\text{H}_5)_2$; solvent, CH_2Cl_2 ; temp, -10°C .

Table II
Copolymerizations of 2-Bu-DOP and DOL

[comonomer], M		DOL, mol fractn in feed	time, h	conversn, %	DOL, mol fractn in copolymer
DOL	2-Bu-DOP				
5.76	1.28	0.82	30	5	0.46
3.53	0.85	0.81	24	4	0.40
5.42	2.04	0.73	15	8	0.35
3.79	1.90	0.67	5	8	0.31
2.83	2.54	0.53	3	9	0.25
1.36	2.54	0.35	3	5	0.15
0.74	2.54	0.22	12	7	0.11

the experimental T_g perfectly. Therefore, the two monomers copolymerize randomly.

The range of composition of the 2-Bu-DOP/DOL copolymer is not as great as that of the THF copolymers. However, the T_g values for the available copolymers agree well with the Fox equation (Figure 8). Therefore, they are random copolymers are well.

The variation of DOL in copolymer versus its amount in feed is plotted in Figure 12. Figure 13 contains similar plots for THF copolymers. These results were analyzed by the method of Fineman and Ross,¹³ who casted the copolymerization equation into the form

$$F(f-1)/f = r_1 F^2/f - r_2 \quad (4)$$

where $f = m_1/m_2$, $F = M_1/M_2$, and m_i and M_i are the mole fractions of the i th monomer in the product and feed respectively. Figures 14 and 15 are the Fineman-Ross plots for the 2-Bu-DOP/DOL and 2-Bu-DOP/THF copolymerizations, respectively. The reactivity ratios and apparent rate constants thus obtained are given in Table VI.

In the present copolymerizations, each chain having terminal A or B monomers units can exist as both cyclic oxonium and alkoxycarbenium ions denoted by superscripts o and c, respectively. Their equilibria can be written as



At temperatures far below T_c , the propagation reactions are





Figure 6. ^1H NMR spectrum of poly(0.75 2-Bu-DOP-co-0.25 DOL).

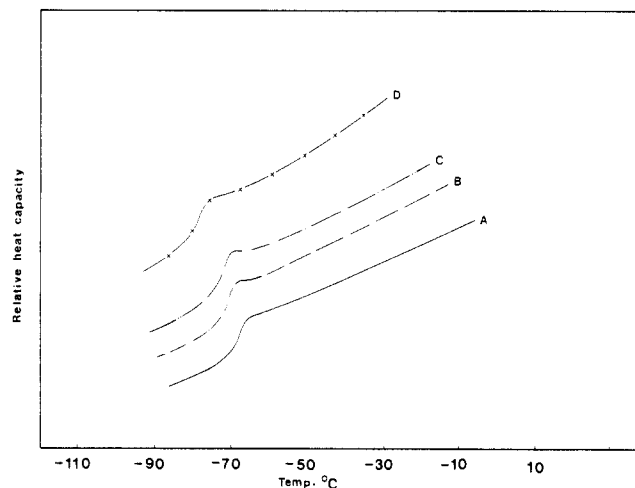


Figure 7. DSC curves: (A) poly(2-Bu-DOP); (B) poly(0.85 2-Bu-DOP-co-0.15 DOL); (C) poly(0.75 2-Bu-DOP-co-0.25 DOL); (D) poly(0.6 2-Bu-DOP-co-0.4 DOL).

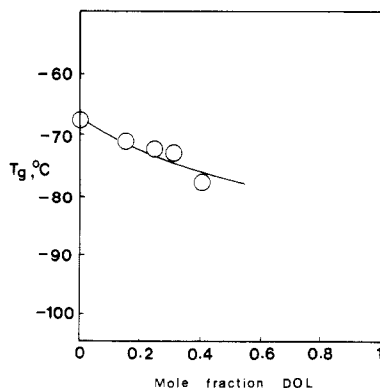


Figure 8. T_g of 2-Bu-DOP/DOL copolymers versus composition. The curve is for the Fox relationship.

In this paper monomer A corresponds to 2-Bu-DOP and monomer B is either DOL or THF. The new oxonium ions formed equilibrate according to eq 5 and 6. It can be shown that the form of the Mayo copolymerization

Table III
Copolymerizations of 2-Bu-DOP and THF at -10°C^a

[comonomers], mol $\times 10^2$		THF, mol fractn in feed	time, h	conversn, %	THF, mol fractn in copolymer
THF	2-Bu-DOP				
7.64	1.09	0.88	22	1.5	0.62
6.93	1.39	0.83	25	2	0.53
5.55	1.85	0.75	23	5	0.38
4.99	2.53	0.66	16	3	0.21
3.50	2.28	0.61	10	7	0.20
3.12	3.17	0.50	7	6	0.12
3.17	3.13	0.50	13	21	0.13
1.89	3.80	0.32	6	5	0.08
1.19	3.12	0.20	2	10	0.05
0.73	3.53	0.17	2	15	0.06

^a Conditions: catalyst, $\text{BF}_3 \cdot \text{O}(\text{C}_2\text{H}_5)_2$; solvent, CH_2Cl_2 ; temp, -10°C .

Table IV
Copolymerization of 2-Bu-DOP and THF at 0°C^a

[comonomer], mol $\times 10^2$		THF, mol fractn in feed	time, h	conversn, %	THF, mol fractn in copolymer
THF	2-Bu-DOP				
6.93	1.40	0.83	25	2.0	0.55
6.34	1.91	0.77	20	2.2	0.42
4.99	2.54	0.66	15	4.2	0.34
3.13	3.16	0.50	7	7.0	0.19
1.93	3.80	0.34	2	11.1	0.13
1.15	3.16	0.27	2	15.0	0.09

^a Conditions as in Table IV, except temperature at 0°C .

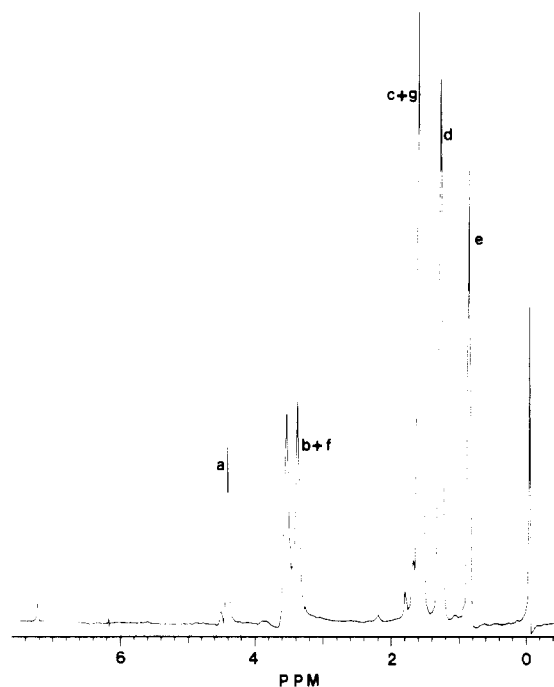


Figure 9. ^1H NMR spectrum of poly(0.8 2-Bu-DOP-co-0.2 THF).

equation is unchanged if the reactivity ratios are redefined in terms of k^o 's and k^c 's

$$r_a = \frac{k_{aa}^o + k_{aa}^c K_A}{k_{ab}^o + k_{ab}^c K_A} = \frac{k_{aa}}{k_{ab}} \quad (15)$$

$$r_b = \frac{k_{bb}^o + k_{bb}^c K_B}{k_{ba}^o + k_{ba}^c K_B} = \frac{k_{bb}}{k_{ba}} \quad (16)$$

The rate constants without superscripts are the experimentally determined values in Table VI. The determination of the individual k^o 's and k^c 's would be a really formidable and arduous task.

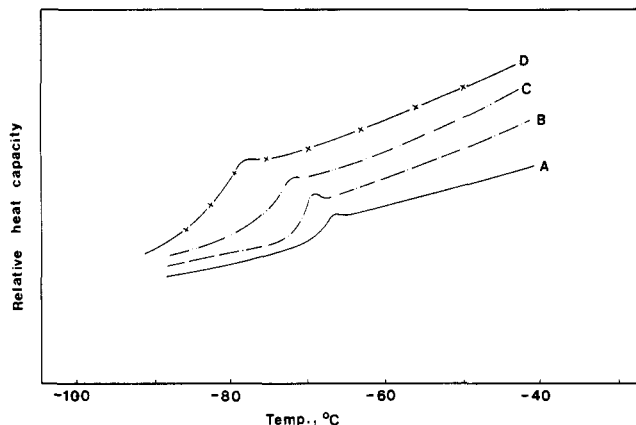


Figure 10. DSC curves: (A) poly(2-Bu-DOP); (B) poly(0.81 2-Bu-DOP-co-0.19 THF); (C) poly(0.62 2-Bu-DOP-co-0.38 THF); (D) poly(0.38 2-Bu-DOP-co-0.62 THF).

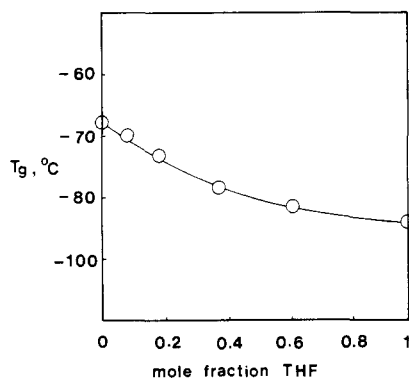


Figure 11. T_g of 2-Bu-DOP/THF copolymers versus composition. The curve is for the Fox relationship.

Table V
Glass Transition Temperatures (°C) for 2-Bu-DOP/THF Copolymers

THF mol fraction in copolymers	T_g obsd by DSC	T_g calcd with Fox eq 2
0	-67.7	-67.7
0.08	-69.8	-69.6
0.19	-73.2	-72.1
0.38	-77.2	-76.4
0.62	-82.7	-81.4
1.0	-89.0	-89.0

Let us first consider the evidence that led Penczek et al.¹ to conclude that the cationic polymerization of DOL proceeds via the O^+ mechanism. They used methoxymethyl cation (I), dimethoxymethane (II), and the adduct of I and II (III) as the models for C^+ , substrate, and O^+ , respectively. The equilibrium constant for $[III]/[I]$ was found to be 3×10^3 M in liquid SO_2 at $-70^\circ C$. Furthermore, Penczek and Szymanski¹⁴ used dynamic NMR line broadening to estimate the rate constants for the addition of II to model ions I and II to be 2×10^6 and 1.9×10^4 (M s)⁻¹, respectively. Under these conditions, even though C^+ is much more reactive than O^+ ; the latter is favored over the former by a factor of 30 as the propagating species by virtue of the difference in concentrations of the ionic species. In the case of 2-Bu-DOP the greater stabilizing effect of the butyl substituent on the alkoxy-carbenium ion than it has on the cyclic oxonium ion suggests a significant decrease in the equilibrium constant to increase $[C^+]$. Since 2-Bu-DOP is a stronger nucleophile than DOL, then the former should homopolymerize much faster via the C^+ mechanism⁷ if the latter propagates by the O^+ mechanism as sug-

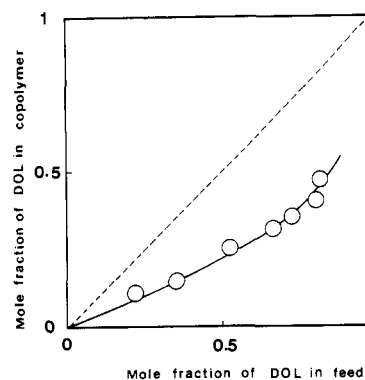


Figure 12. Mole fraction of DOL in copolymer versus in feed.

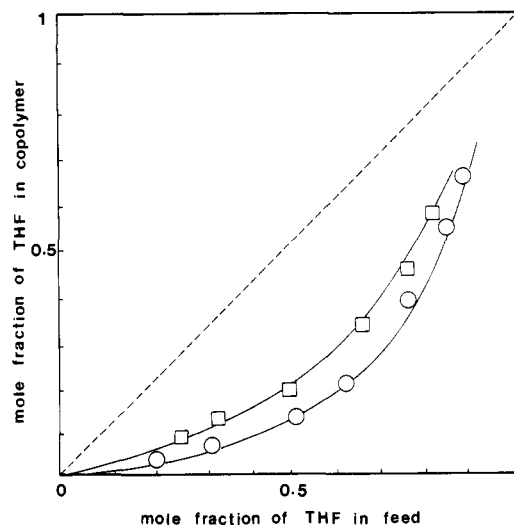


Figure 13. Mole fraction of THF in copolymer versus in feed for 2-Bu-DOP/THF copolymerizations: (O) at $-10^\circ C$; (\square) at $0^\circ C$.

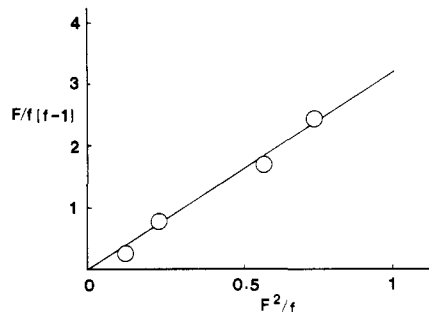


Figure 14. Fineman-Ross plot for 2-Bu-DOP/DOL copolymerizations at $-10^\circ C$.

gested.¹ The results of this study showed the two monomers to have the same values for the rate constant of propagation. Furthermore, the value of k_{ba} is only 60% larger than k_{ab} instead of the much larger difference suggested by the estimated rate constants for the model systems. In these qualitative considerations the counter effects of nucleophilicity and steric hindrance for the two monomers may be mutually compensatory.

Since our experimental conditions are very different from those used to estimate concentrations and reactivities of the ionic species and choice between mechanistic pathways for complex chemical processes cannot be made unambiguously on the basis of experimental results, we thought computational chemistry may be useful to clarify matters. The results of an AMI computational study using restricted Hartree-Fock wave functions of the cationic polymerization mechanism of cyclic acetals have been

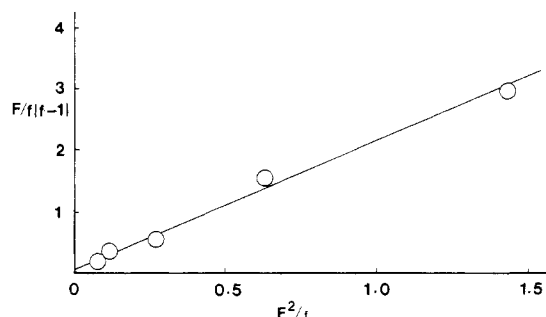


Figure 15. Fineman-Ross plot for 2-Bu-DOP/THF copolymerizations at 0 °C.

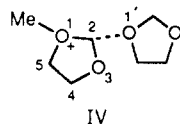
Table VI
Copolymerization Kinetic Parameters with 2-Bu-DOP

	comonomer		
	DOL	THF	
temp, °C	-10	-10	0
r_a	2.13 ± 0.05	5.1 ± 0.04	3.3 ± 0.03
r_b	0.12 ± 0.05	0.08 ± 0.02	0.11 ± 0.04
$r_a r_b$	0.26	0.41	0.36
$k_{a,a}$ (M s) ⁻¹	7.1×10^{-4}		3.0×10^{-3}
$k_{b,b}$ (M s) ⁻¹	6.5×10^{-4}		8.2×10^{-5}
$k_{a,b}$ (M, s) ⁻¹	3.3×10^{-4}		9.1×10^{-4}
$k_{b,a}$ (M, s) ⁻¹	5.4×10^{-4}		7.4×10^{-4}

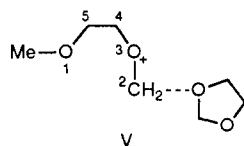
obtained;¹⁵ they are in fairly good agreement with the results of Penczek and co-workers.^{1,14}

The enthalpy changes for ring opening, $\Delta H^\circ_{\text{rxn}}$, of six cyclic acetals have been calculated. The results summarized in Table VII showed no strong dependence of $\Delta H^\circ_{\text{rxn}}$ on the ring size. On the other hand, there are very large decreases of $\Delta H^\circ_{\text{rxn}}$ due to alkoxy substituent at the C(2) carbon. In the case of DOL, $\Delta H^\circ_{\text{rxn}} = +3.9$ kcal mol⁻¹. If $\Delta S^\circ_{\text{rxn}}$ is small, then the gas-phase prediction for $[C^+]/[O^+] \sim 10^{-3}$ is comparable to that estimated by Penczek et al.¹ When one compares DOL with 2-Me-DOL, then the difference between $\Delta H^\circ_{\text{rxn}}$ is -10.3 kcal mol⁻¹. Since the $T\Delta S^\circ_{\text{rxn}}$ should be comparable for the ring opening of the two molecules, the $[C^+]/[O^+]$ ratio is greater by 3×10^7 -fold with the 2-Me substituent as without. The computational results leave no doubt that the open alkoxy-carbenium ion is the dominant species in the cationic polymerization of cyclic acetals.

The activation energies have also been computed¹⁵ for the formation of the oxonium ion substitution ring-opening transition state for the O⁺ mechanism



and of the carbenium ion addition transition state for the C⁺ mechanism



The formation of IV involves a sharply rising barrier as O(1') approaches within 2.1 Å of the C(2) atom. The overall $E_a \sim 4.9$ kcal mol⁻¹ at a C(2)-O(1') transition distance of 2.34 Å. The formation V in the C⁺ mechanism shows only a gentle rise to an $E_a \sim 1.3$ kcal mol⁻¹

Table VII
Heats of Formation and Enthalpy Change for Ring Opening

cyclic acetal	heat of formation, kcal mol ⁻¹		$\Delta H^\circ_{\text{rxn}}$, kcal mol ⁻¹
	oxonium ion	carbenium ion	
DOL	97.3	101.2	+3.9
2-Me-DOL	90.6	84.2	-6.4
DOP	79.9	84.4	+4.5
2-Me-DOP	75.3	68.1	-7.2
TOC	47.7	52.5	+4.8
2-Me-TOC	42.3	39.5	-2.8

at a C(2)-O(1') distance of 2.28 Å. Thus, the AMI computed activation energy difference contribution to k_p at 263 °C is ca. 10^3 greater for the C⁺ mechanism than the O⁺ mechanism. According to these calculations there is no difference in the relative rates of dioxolane polymerization, for the two mechanisms, i.e. $[C^+]/[O^+]k_p^\circ \sim 1$.

The fact that all the k 's in Table VI for dioxolane copolymerization differ less than a factor of 2 can be interpreted as propagation via C⁺ mechanism for both monomers. The $\Delta H^\circ_{\text{rxn}}$ for ring opening of dioxolane may be more negative than the value given in Table VII; and the rate constant for the ring opening of dioxolane O⁺ to form C⁺ is estimated¹⁴ to be 1.9×10^4 s⁻¹ by NMR line-broadening measurements¹⁴ (vide supra).

The homopolymerization rate constant for THF is much smaller than that for 2-Bu-DOP. This is attributable to the lower nucleophilicity of THF and lower reactivity of its O⁺. The copolymerization results are 10-fold greater in value of $k_{a,b}$ than $k_{b,b}$ is due to the higher reactivity of O⁺ toward 2-Bu-DOP. Conversely, the lowering of $k_{b,a}$ compared to $k_{a,a}$ may be the result of lower reactivity of C⁺ toward THF. The chains with THF terminus must be in the oxonium ion state because there is no α -oxygen to stabilize a carbenium ion.

In conclusion, the copolymerizations of 2-Bu-DOP with THF gave results consistent with propagating species having the C⁺ or O⁺ structure depending upon whether the last added monomer is 2-Bu-DOP or THF, respectively. The copolymerization data of 2-Bu-DOP with DOL can be interpreted as propagation predominantly via the C⁺ mechanism. AMI computation showed that DOL propagation can proceed also through the O⁺ mechanism.

Acknowledgment. This was supported by a grant from the Office of Naval Research.

References and Notes

- (1) Penczek, S.; Kubisa, P.; Matyjaszewski, K. *Adv. Polym. Sci.* **1980**, *37*, 1.
- (2) Cordes, E. H. In *Progress in Physical Organic Chemistry*; Streitwieser, A., Tafts, R. W., Eds.; Interscience: New York, 1967; Vol. 4, p 1.
- (3) Dainton, F. S.; Irin, K. J. *Trans. Faraday Soc.* **1950**, *46*, 331.
- (4) (a) Skuratov, A. A.; Strepikheev, A. A.; Shtekher, S. M.; Volokhina, A. V. *Dokl. Akad. Nauk SSSR* **1957**, *117*, 263. (b) Yamashita, Y.; Okada, M.; Suyama, K.; Kasahara, H. *Macromol. Chem.* **1960**, *114*, 146. (c) Plesh, P. H.; Westermann, P. H. *Polymer* **1969**, *10*, 105. (d) Kozub, L. I.; Markevich, M. A.; Berlin, A. A.; Yenikolopyan, N. S. *Vyrokamol. Soedin* **1968**, *10*, 2007.
- (5) (a) Okada, M.; Mita, K.; Sumitomo, H. *Makromol. Chem.* **1973**, *163*, 225. (b) Okada, M.; Hisada, T.; Sumitomo, H. *Makromol. Chem.* **1978**, *179*, 959.
- (6) (a) Okada, M.; Yagi, K.; Sumitomo, H. *Makromol. Chem.* **1973**, *163*, 225. (b) Okada, M.; Hisada, T.; Sumitomo, H. *Makromol. Chem.* **1978**, *179*, 959.
- (7) Chien, J. C. W.; Cheun, Y. G.; Lillya, C. P. *Macromolecules* **1988**, *21*, 870.

- (8) Yamashita, Y.; Maymi, J.; Kawakami, Y.; Ito, R. *Macromolecules* **1980**, *13*, 1075.
 (9) Xu, B.; Lillya, C. P.; Chien, J. C. W. *Macromolecules* **1987**, *20*, 1445.
 (10) (a) Finat, Y.; Plesch, P. H. *J. Polym. Sci., Polym. Lett. Ed.* **1975**, *13*, 135. (b) Okada, M.; Mita, K.; Sumitomo, H. *Makromol. Chem.* **1975**, *179*, 859. (c) Finat, Y.; Plesch, P. H. *Makromol. Chem.* **1975**, *176*, 1179.
 (11) Astle, M. J.; Zastowsky, J. A.; Lafyatis, P. G. *Ind. Eng. Chem.* **1969**, *127*, 271.
 (12) Fox, J. F. *Am. Phys. Soc.* **1956**, *1*, 123.
 (13) Fineman, F.; Ross, S. D. *J. Polym. Sci.* **1950**, *5*, 259.
 (14) Penczek, S.; Szymanski, H. *Polym. J.* **1980**, *12*, 617.
 (15) Lahti, P. M.; Lillya, C. P.; Chien, J. C. W., accepted for publication.

Room Temperature Polyesterification

Jeffrey S. Moore and Samuel I. Stupp*

Department of Materials Science and Engineering, University of Illinois at Urbana—Champaign, Urbana, Illinois 61801. Received January 24, 1989; Revised Manuscript Received May 22, 1989

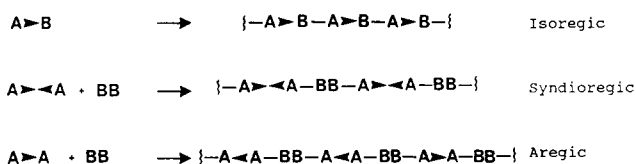
ABSTRACT: A new room temperature polymerization method has been developed for the synthesis of high molecular weight polyesters directly from carboxylic acids and phenols. The solution polymerization reaction proceeds under mild conditions, near neutral pH, and also avoids the use of preactivated acid derivatives for esterification. The reaction is useful in the preparation of isoregic ordered chains with translational polar symmetry and also in the polymerization of functionalized or chiral monomers. The conditions required for polymerization in the carbodiimide-based reaction included catalysis by the 1:1 molecular complex formed by 4-(dimethylamino)pyridine and *p*-toluenesulfonic acid. These conditions were established through studies on a model system involving esterification of *p*-toluic acid and *p*-cresol. Self-condensation of several hydroxy acid monomers by this reaction has produced routinely good yields of polyesters with molecular weights greater than 15 000. It is believed that the high extents of reaction required for significant degrees of polymerization result from suppression of the side reaction leading to *N*-acylurea. The utility of this reaction in the formation of polar chains from sensitive monomers is demonstrated here by the polycondensation of a chiral hydroxy acid.

Introduction

Polymerization by condensation reactions has several synthetic limitations which include lack of methodologies for precise control of chain length and few known reactions that take place under extremely mild conditions. This last limitation is an obstacle to synthesis of high molecular weight products from sensitive monomers that are functionalized or chiral. A related problem is the general need to convert condensation monomers to an activated derivative prior to polymerization. This precludes the direct self-condensation of "A-B" type monomers, important in the formation of isoregic polymers that have translational polar symmetry. The term isoregic is used in this manuscript to describe a form of regiochemical order, specifically that of a chain with molecular direction. This term was adapted from the definitions of Cais and Sloan¹ describing directional isomerism (regioisomerism) in vinyl polymers. As illustrated in Scheme I, condensation polymers derived from A-B monomers form chains with isoregic order. Synthetic access to this class of chain structures is only possible through this type of monomer and therefore methodologies of broad scope for its polymerization are essential. We report here on a new polymerization method, which yields high molecular weight polyesters at room temperature directly from carboxylic acids and phenols under extremely mild conditions.

Although several reactions have been developed for direct condensation of acids and amines leading to polyamides,² few methods currently exist to construct polyesters directly from unactivated monomers. Melt-phase

Scheme I Regiochemical Order in Condensation Polymers



transesterification has been used extensively although reaction temperatures greater than 250 °C are generally required to obtain high molecular weight polymers. The high temperatures employed prevent application of this reaction to the polymerization of monomers that contain sensitive functional groups. Also, if ester bonds preexist in the monomer, transesterification will lead to sequentially random polymer chains.³ Recently, solution procedures for direct polyesterification have been reported by Higashi et al.⁴ One of these procedures involves in situ activation of carboxylic acids with diphenyl chlorophosphate,^{4a} while a second procedure employs arylsulfonyl chloride condensing agents.^{4b-d} These reactions are carried out in pyridine at temperatures near 120 °C. In our experience, the method based on arylsulfonyl chloride reagents leads to undesirable phenyl tosylates as a significant side product and hence gives low molecular weight polymers. Moreover, use of milder conditions such as lower reaction temperatures gives increasing amounts of tosylate ester side products. When the mixed anhydride is allowed to form before the diphenol is introduced, good results can be obtained. This modi-